Journal of Power Sources 212 (2012) 130–138

Contents lists available at SciVerse ScienceDirect

Journal of Power Sources

journal homepage: www.elsevier.com/locate/jpowsour

Comparing batteries to generators as power sources for use with mobile robotics

Drew G. Logan [a], Jesse Pentzer [a], Sean N. Brennan [a,*], Karl Reichard [b]

[a] Department of Mechanical and Nuclear Engineering, The Pennsylvania State University, University Park, PA 16802, United States
[b] Applied Research Laboratory, The Pennsylvania State University, University Park, PA 16802, United States

ARTICLE INFO

Article history:
Received 25 October 2011
Received in revised form
12 March 2012
Accepted 13 March 2012
Available online 13 April 2012

Keywords:
Robot
Allometry
Generator
Battery

ABSTRACT

This paper considers the scaling principles associated with the power and energy density of batteries and generators as applied to mobile robots and similarly-sized vehicles. We seek to identify, based on present technology, the size range at which a generator inclusive of a direct current electric motor, gearbox, and internal combustion engine can be effectively used to replace modern batteries. Models were derived to scale each component of the generator as a function of power, mass, efficiency, and speed. For a given power, energy, or mass requirement, these models illustrate that generators based on conventional technology are ill-suited for smaller robots. The results indicate that there is an intermediate robot size above which a hybrid generator/battery architecture is desirable. Using these scaling principles with modest extensions of existing battery technologies, it is also possible to infer the near-future performance of robot power technology and thus illustrate whether the generator-versus-battery tradeoff will shift toward or away from a hybrid robot topology for smaller vehicle systems.

1. Introduction

There is great interest in extending to mobile robots the capabilities of a hybrid vehicle: to refuel quickly, to switch seamlessly between electrical and internal combustion power sources, and to have an extremely long runtime. However, there is a disconnect between the power system used in a traditional gasoline powered internal combustion (IC) engine moving a 2000 kg automobile at highway speeds versus a 10 kg to 50 kg mobile robot driven by electric motors and batteries. The focus of this research was to determine the point(s) where a generator and a battery have equivalent energy and power on a per-mass basis, and thereby discriminate the size at which generators would be a beneficial replacement to a battery, all costs aside.

The interest in hybrid robot technology arises from the desire to extend operating time/range and the greater energy density of liquid fuel sources compared to batteries. For example, diesel fuel has an energy density of 46 MJ/kg which is nearly 64 times the energy density of the leading lithium ion battery at 0.72 MJ/kg [1]. Even though diesel has such a high energy density, what is unclear is whether the components that convert this chemical energy to electrical energy – an internal combustion engine, a gearbox, and an electrical generator – will be so large that the effective energy density of the resulting system is better or worse than the battery being replaced. This study compares the power and energy available from a battery versus a generator while enforcing a mass equivalence between the two systems, across different size scales.

There has been some prior research examining the scaling limitations of robotic drivetrains. For example, it is well known that below a certain physical size, mobile ground robots no longer fall within the domain of classical physics [2,3]. More specifically, Caprari et al. have examined how power required for motion changes as a function of the robot platform size [3]. Their research into scaling lower limits of electromagnetic motors showed a positive linear correlation between volume and power [3]. Madden compared the relative benefits and drawbacks of using combustion engines, actuators, and other mechanical devices in place of electric motors as a means to create a similar power density to that seen in human muscle. In his work, he found that the energy density of gasoline is "20 times that of a good battery" but is primarily useful for continuous power draws and not in a muscle-like situation where there is a high switching rate in the amount of power required [4]. Other research has shown that both electric motors and IC engines have a maximum force in newtons, F, that scales with mass in kilograms, M, to the first power as seen in (1) [5].

$$F = 55(M)^{0.999} \tag{1}$$

Maximum force for rotary electric motors was defined to be the maximum steady-state torque output of the motor divided by the output shaft radius. This correlation was shown to be true up to motors as large as 4 kg [5].

* Corresponding author. Tel.: +1 814 863 2430; fax: +1 814 865 9693.
E-mail address: sbrennan@psu.edu (S.N. Brennan).

0378-7753/$ – see front matter © 2012 Elsevier B.V. All rights reserved.
doi:10.1016/j.jpowsour.2012.03.041

Additionally, research into Hybrid Electric Vehicles (HEVs) has sought to determine the usable upper size limits of DC motors and to determine the feasibility of replacing IC engines with hybrid electric drivetrains. Within such vehicle applications, the feasibility of hybrids is examined by comparing road load characteristics and the performance analysis of electric motor drivetrains [6]. Many of the losses associated with DC motors become limiting as the DC motor increases in size and power. Copper loss, for example, is proportional to the motor current squared [7] and thus heat dissipation places an upper limit on the practical size of DC motors.

Huei Peng et al. have performed extensive research into subsystem scaling, power management, and design optimization of hybrid electric vehicles with varied powertrain configurations [8–10]. In doing so, scaling principles were derived for electric motors, IC engines, fuel cells, batteries, and hydraulic drivetrains to scale each as a function of power. System modeling for each has involved the utilization of Simulink, Vehicle System Modeling (VESIM), and first principles physics-based modeling [8–10].

This paper presents a derivation of the scaling rules which predict the mass-to-power and mass-to-energy curves of electrical generators, gearboxes, and internal combustion engines suitable for mobile robots. Using these relationships, we identify the portion of the design space in which generators are a more mass-efficient energy source than batteries. Other work in this area generally focuses on powertrains for passenger size vehicles. The work presented here provides a design tool useful when choosing powertrain components for mobile robots. Articles addressing battery/generator comparisons at a similar scale exist [11,12], but have not been published in peer reviewed literature nor do they explain the underlying factors that drive the power scaling laws.

The remainder of this paper is outlined as follows. Section 2 discusses work in allometric design for both robotics and hybrid power systems. Section 3 covers the scaling theory of the subsystem components of the generator as well as the method derived to efficiently scale the generator system. Section 4 presents the results of how the specific power and energy of a generator scale relative to a BB2590 battery. Section 5 discusses a comparison of generators and batteries on an energy-per-mass basis, and Section 6 presents the results of adjusting generator and battery properties to predict future performance. Section 7 describes the energy storage and power output of a system composed of a generator and battery, and Section 8 discusses the conclusions drawn from this work.

2. Allometry of hybrid powertrain components

Hybrid powertrains generate power onboard a vehicle using a combination of energy conversion technologies. The energy generation components in the most basic functional form consist of a liquid chemical energy source (diesel fuel is assumed hereafter, though this is readily changed in the methods described later), an IC engine to convert chemical energy into mechanical energy, a device hereafter referred to as an electrical generator to convert mechanical motion into electrical energy, and finally a gearbox that changes the shaft rotational velocity from the IC engine to the appropriate speed for the electrical generator. Each of these components has a mass that changes as a function of power, energy, speed, and/or efficiency. Because each component has a different size per unit mass or power, the overall generator will have a power-to-mass ratio that changes as a function of physical size. The analysis of how performance changes with size is known as "allometry", and this section develops allometric predictions for each generator component.

To develop these predictions, this research utilized extensive previous work that examined the scalability and limits of electric motors, gearboxes, and IC engines independently. This previous research did not consider all of these components working together as a generator, and thus a key contribution of this paper is to combine these previous theories into a formal method to create the most mass-efficient generator system and compare the result to various battery technologies. Some generator details are ignored to simplify the analysis, for example that the generator might need to carry a battery system for non-manual starting, that the frame of the robot or vehicle may have to be reinforced to support generator vibration, etc.

2.1. Electrical generator modeling

A general DC motor electric circuit was the starting point for modeling a DC motor operating as an electrical generator. The input voltage is replaced with a load resistance, R_L, and the input to the system is the angular speed of the armature, ω. It is then possible to solve for the current produced by the generator, i, as

$$i = \frac{V_{emf} - V_b}{R_a + R_L} = \frac{K\omega - V_b}{R_a + R_L}, \tag{2}$$

where V_{emf} is the back-EMF voltage, V_b is voltage loss across the commutator brushes, R_a is the armature resistance, and K is the motor back-EMF constant.

The mechanical side of the motor was modeled as a simple rotational system. Equating the acting torques to the angular acceleration of the motor, $\dot{\omega}$, yields

$$J\dot{\omega} = T_{in} - b\omega - Ki - T_f \tag{3}$$

where J is the rotational inertia of the motor, T_{in} is the torque input to the motor from the IC engine, b is the viscous damping coefficient for the motor, and T_f is the constant friction torque for the motor. At steady state, $\dot{\omega} = 0$ and solving for T_{in} gives

$$T_{in} = b\omega + K\frac{K\omega - V_b}{R_a + R_L} + T_f \tag{4}$$

where (2) has been substituted for the current, i, in (3). Using (2) and (4) it is possible to solve for the power produced by the electrical generator as

$$P_{out} = i^2 R_L = \frac{\left(V_{emf} - V_b\right)^2}{\left(R_a + R_L\right)^2} R_L \tag{5}$$

and for the power input to the electrical generator as

$$P_{in} = T\omega = b\omega^2 + K\omega\frac{K\omega - V_b}{R_a + R_L} + T_f\omega. \tag{6}$$

The efficiency of the electrical generator, η, is then the ratio of output power to input power.

Using this model, the performance of an electrical generator can then be characterized as shown in Fig. 1. To create the curves, the electrical generator was spun at no-load speed while the load resistance was varied. The no-load speed was chosen because the power output of the electrical generator increases with higher speeds, as shown in (5). For maximum output power at a given load resistance, the electrical generator should spin as fast as possible, and it was assumed that the no-load speed was the maximum safe speed of the electrical generator.

For this research it was important to know the peak efficiency of the electrical generator and the power output at peak efficiency. The electrical generator model was compared to manufacturer data for DC motors to see if allometric DC motor scaling laws could be

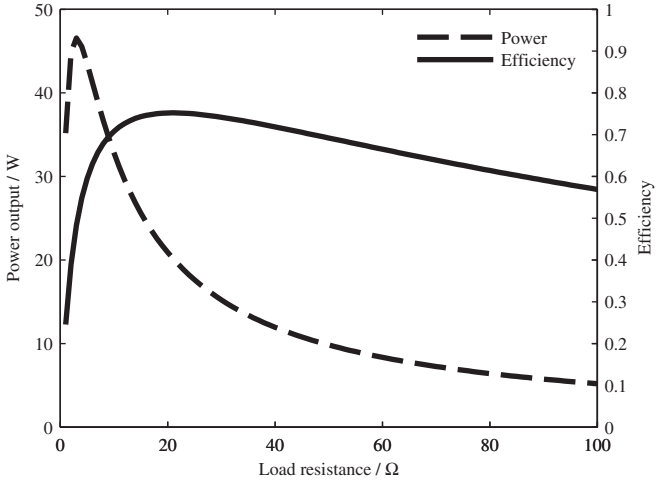

Fig. 1. Representative performance curves of DC motor operating as an electrical generator. A Pittman 9234S006 was modeled to create the curves [13].

used to predict electrical generator performance. Vendors measure and report the performance of the DC motors being driven electrically as a motor rather than an electrical generator. Allometric models therefore cannot be easily built using vendor data for DC motors acting as electrical generators. Scaling laws for commercial diesel generators have been recently published, but all generators used in developing the scaling laws were over 100 kg, much larger than the systems considered in this work and not practical for ground robots [14].

Comparing the theoretical performance of an electrical generator with vendor-supplied values of DC motor performance shows that the performance of each can be approximated as equivalent. In Figs. 2 and 3, vendor-supplied values of motor maximum efficiency and power output at maximum efficiency are plotted against predicted values of generator maximum efficiency and generator power output at maximum efficiency. The data in Fig. 2 is clustered between 60% and 80% efficiency, and the electric motors on the scale studied in this work generally operate with a maximum efficiency in this range. The solid line with slope of one represents perfect agreement in motor and generator performance values. The

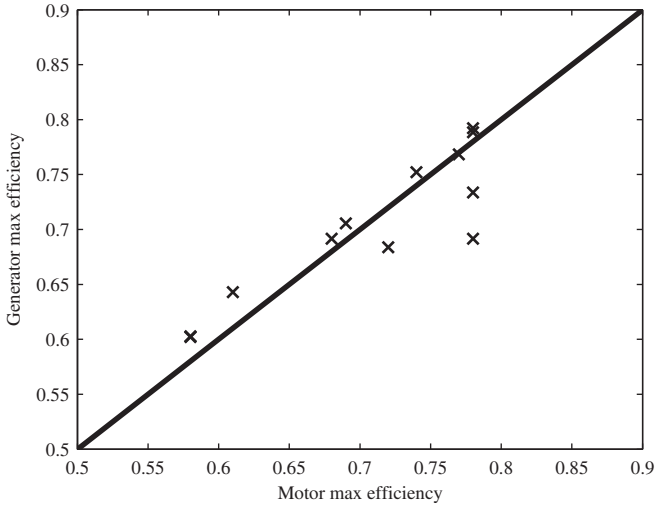

Fig. 2. Comparison of motor maximum efficiency and electrical generator maximum efficiency.

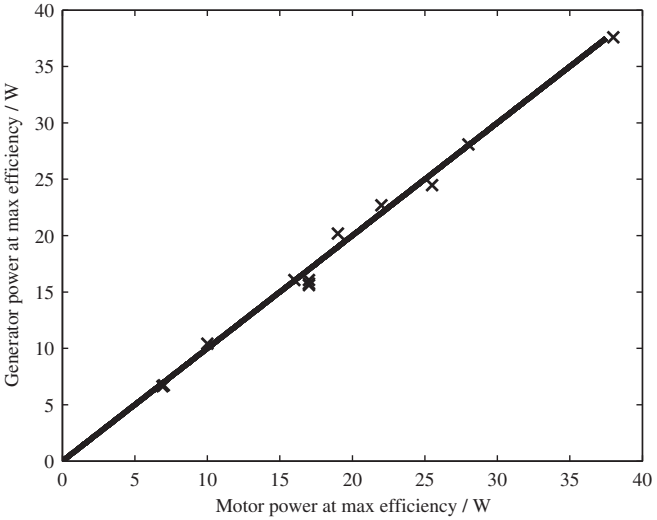

Fig. 3. Comparison of motor power at maximum efficiency and electrical generator power at maximum efficiency.

results indicate that the peak efficiency and power produced at peak efficiency are approximately the same for a DC motor acting as a motor or as an electrical generator.

The similarities in efficiency and power output of DC motors operating as electrical generators and motors allows scaling laws for DC motor parameters to be used. These scaling laws are functions of only the power output of the motor when operating at peak efficiency.

To develop a model of DC motor performance, Kenjo and Nagomori derived equations using first principles of physics that predict steady-state characteristics of brushed DC motors [15], equations that are summarized here. The power, torque, and efficiency of a motor, as seen in Fig. 4, can be predicted as a function of the motor speed when the following characteristics are known: rated voltage, no-load current and speed, torque constant, armature resistance, and peak power output. The predicted performance agrees extremely well with vendor-supplied data. Kenjo and Nagamori used the circuit shown in Fig. 5 to determine motor performance at steady state. The steady state efficiency is given by

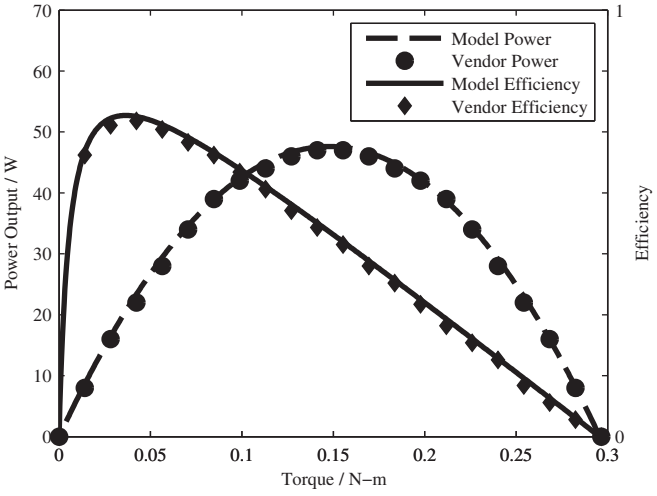

Fig. 4. Representative performance curves of Pittman 9234S006 DC motor [13].

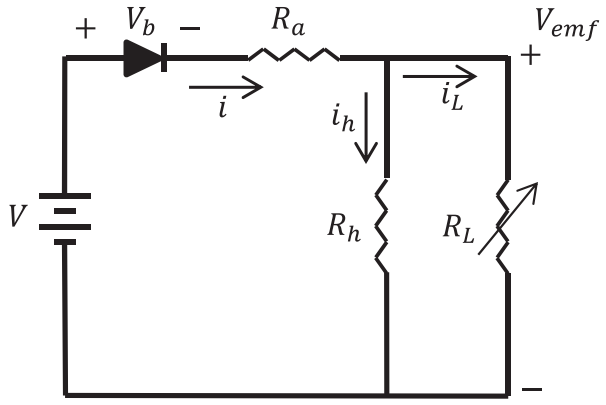

Fig. 5. Steady state DC motor circuit.

$$\eta = \frac{V_{\text{emf}}}{V} - \frac{R_{\text{a}}}{R_{\text{h}}}\frac{V_{\text{emf}}^2}{V\left(V - V_{\text{b}} - V_{\text{emf}}\right)}. \tag{7}$$

where R_{h} represents windage and mechanical losses. The maximum efficiency is found by solving $\partial\eta/\partial V_{\text{emf}} = 0$ for V_{emf} and then substituting back into (7). Utilizing the motor constant M, defined to be

$$M = \sqrt{\frac{R_{\text{h}} + R_{\text{a}}}{R_{\text{a}}}}, \tag{8}$$

the maximum efficiency can be expressed as

$$\eta_{\max} = \frac{V - V_{\text{b}}}{V}\cdot\frac{M-1}{M+1}. \tag{9}$$

Next, a thorough market survey was conducted to determine representative parameters of modern brushed and brushless DC motors. Using data collected across approximately 110 motors, relationships between motor power at peak efficiency and the motor size, peak operating speed, and peak efficiency were found. Fig. 6 shows a clear positive correlation between the mass of a DC motor, m_{DC}, (in kg) and its operating power at peak efficiency,P (in Watts). The equation of the fit line is

$$m_{\text{DC}} = 1.363(P)^{0.71}, \tag{10}$$

agreeing with power scaling results reported by Marden if speed is constant [5]. The no-load DC motor speed, ω_{o}, is negatively correlated with an increase in the motor's operating power at peak efficiency as shown in Fig. 7. The equation of the fit line is

$$\omega_{\text{o}} = 8877(P)^{-0.116}. \tag{11}$$

Fig. 8 shows a positive correlation between DC motor peak efficiency and power output described by the equation

$$\eta_{\max} = 0.91 - 0.47P^{-0.3}. \tag{12}$$

Scaling laws (10)–(12) were used to determine the ideal DC motor performance for a given output power.

2.2. Gearbox modeling

The allometry of gearboxes was the most difficult to determine. In order to find this information, data on DC motors with factory-installed gearboxes was collected. For each, the peak efficiency of the gearbox and motor in combination was provided by the vendor in addition to a number of motor characteristics. Using the motor characteristics, the peak efficiency of each motor by itself was calculated using (9). The gearbox efficiency, η_{GB}, was then computed as a function of the gearbox ratio, N, using

$$\eta_{\text{GB}} = -0.06\ln N + 0.93. \tag{13}$$

Fig. 9 shows the computed gearbox efficiency as a function of the gearbox gear ratio. These gearbox scaling principles were computed across many different motor characteristics including size, power, speed, and torque. The relationship suggests that the resulting gearbox efficiency is largely independent of physical size. Additionally, these results agree with general estimates of gearbox efficiency provided by Clark and Owings [16].

The mass of a DC motor's gearbox, m_{GB}, was also computed from vendor data. First, the mass of the DC motor by itself was calculated using (10) and subtracted from vendor-reported motor/gearbox data to obtain the gearbox mass. The mass of the gearbox was expressed as

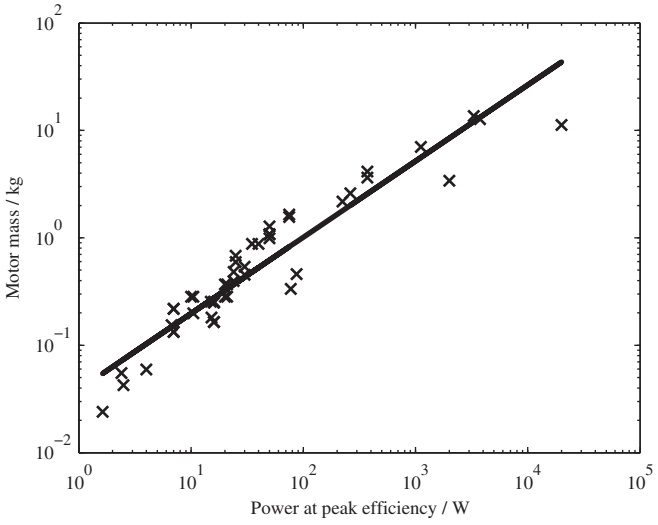

Fig. 6. Power vs DC motor mass at peak efficiency.

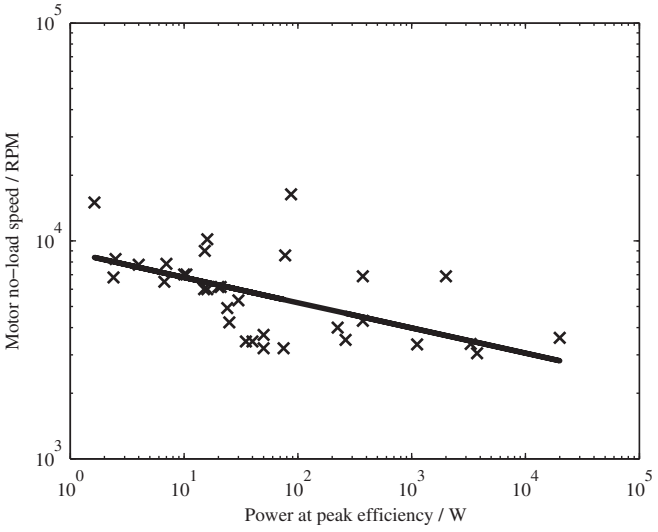

Fig. 7. Power vs DC motor speed at no-load.

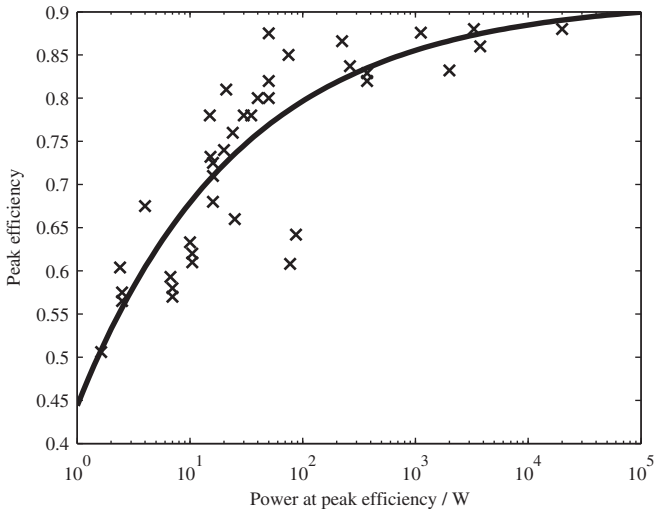

Fig. 8. Power vs DC motor peak efficiency.

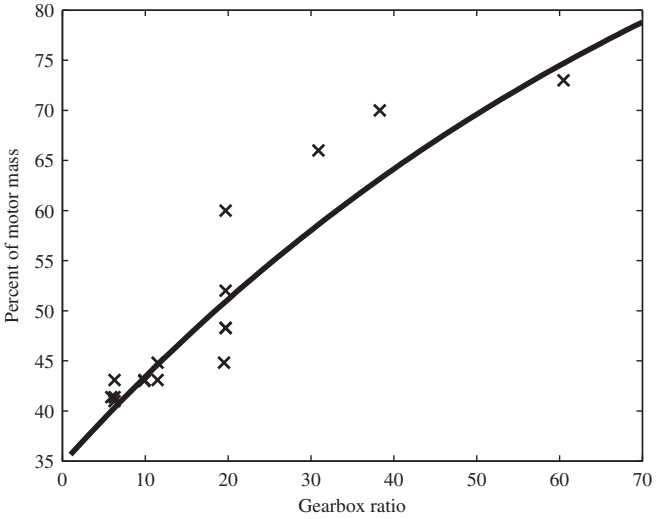

Fig. 10. Percentage of motor mass as a function of gearbox ratio.

$$m_{GB} = m_{DC}\left(1.15 - 0.8e^{-0.012N}\right). \quad (14)$$

The resulting fit is shown in Fig. 10.

2.3. Internal combustion engine modeling

To determine the allometry of internal combustion engines, we utilized previous work on aircraft IC engines where weight versus power is well documented and highly optimized [17]. Figs. 11 and 12 show the correlation between power, mass, and speed for internal combustion engines independent of motor characteristics such as number of engine strokes, number of cylinders, fuel type, engine displacement, etc. This data and additional detail can be found in McMahon and Bonner [17].

2.4. Battery modeling

Finally, the battery itself is subject to scaling laws. In this work, we assumed that the battery size and scaling is achieved by adding "more of the same", to create packs of similarly-sized batteries. As a base unit, a common, self-contained, high-production, high-performance battery system was desired. For this reason, we used a military-grade lithium ion BB2590 series battery as the representative sample of a lithium ion technology [18]. Other rechargeable batteries were also considered in this work, but again, the power available was still considered to be a constant scaling factor times the amount of power available from a basic reference battery design.

Primary batteries, which are not rechargeable, were not considered in this work because they are not commonly used as power sources on mobile ground robots. Over the life of a robot, it is not economically feasible to utilize one-time-use primary batteries when currently available lithium ion cells are rated for over 1000 cycles while maintaining 90% capacity. Nevertheless, the approach presented here applies equally to primary and rechargeable batteries, regardless of chemistry. The analysis can simply be repeated with different parameters for battery energy or power density and will simply shift the break-even point in the results as shown in Section 5.

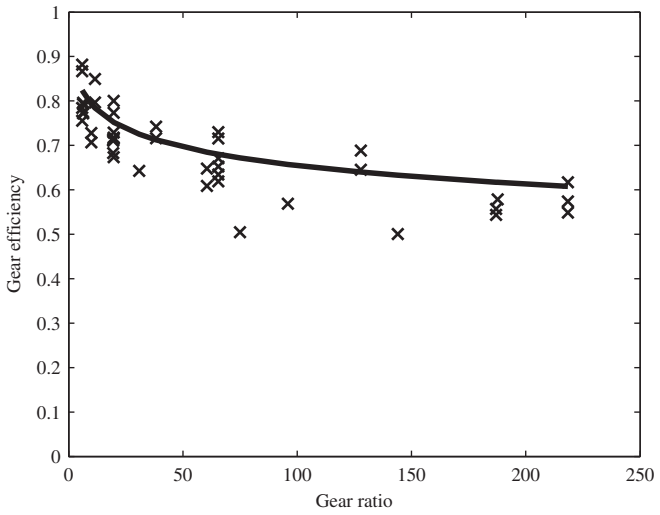

Fig. 9. Gearbox efficiency as a function of gearbox ratio.

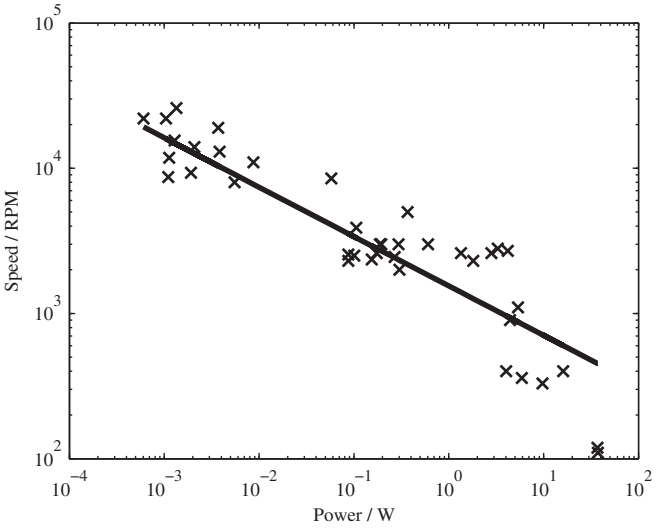

Fig. 11. IC engine speed as a function of the motor power.

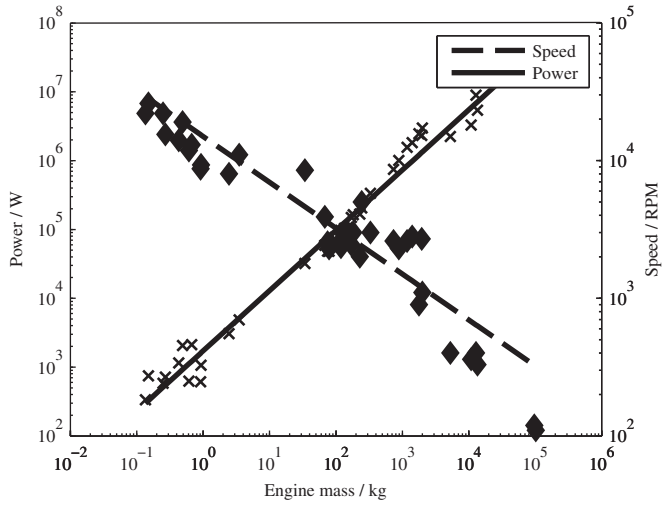

Fig. 12. IC engine power and speed as a function of engine mass.

Another energy storage device not considered here is the ultracapacitor. The addition of ultracapacitors would shift the analysis from one comparing separate power sources to an analysis of power system cycles and control. The control and power cycle issues would arise as ultracapacitors alone are insufficient for robot missions, and thus must be paired with another energy source. Furthermore, ultracapacitors are usually used to provide short-duration, peak electrical power and thus are sized to meet power requirements specific to a particular mission profile. Research on optimal ultracapacitor control or sizing is outside the work presented here.

Another technology not considered in this work is the fuel cell. Ground mobile robots are often power limited, not energy limited. Current battery technology generally provides satisfactory endurance, but mission tasks such as stair climbing require large power draws. A Ragone plot comparing lithium ion batteries to fuel cells shows that the two have similar ranges of specific energy, but that batteries are capable of much higher specific power [19]. Therefore, batteries remain the logical choice between the two for powering mobile robots. Also, it is difficult to develop scaling laws for fuel cells due to the lack of complete fuel cell systems available in the size scales needed for powering a mobile robot. Specifications for individual cells are available from manufacturers, but often these exclude external cooling and air handling systems necessary for operation.

3. Method of generator modeling

The previous scaling principles were combined to create a model to predict the size versus performance tradeoffs of a diesel electric power generator. Rather than attempting many different combinations of motor/gear/engine designs to produce scatter plots of power, a more efficient approach was developed by specifying a required power and iteratively optimizing the associated components accordingly. The process is explained further below.

First, the output power needed from the electrical generator was selected. This output power was used to size the DC motor and determine the maximum efficiency of the motor. Next, to size the gearbox, one must know the power from the IC engine, as well as the input speeds from the IC engine into the gearbox. Both were used to determine the power losses associated with the gearbox. Unfortunately, this resulted in a "circular" calculation, where one must know the gearbox losses to size the IC engine, and one must know the IC engine operating speed to calculate the gearbox losses.

To overcome this problem without a computationally intensive substitution of gearbox equations into IC engine calculations, we instead calculated the gearbox design iteratively. To begin the process, an arbitrary gearbox efficiency of 50% was selected. Using this gearbox efficiency, an IC engine was sized to provide enough power to the DC motor to overcome the losses from the gearbox and provide the requested power. The corresponding IC engine speed was then determined using the correlation between power and speed of an IC engine from Fig. 11. The ratio of the IC motor speed to the DC motor speed at peak efficiency was then calculated, and this specified a new gearbox ratio. This gearbox ratio was used to calculate a gearbox efficiency. This new efficiency was then used to replace the original "guessed" efficiency, and the design process was repeated until the gearbox design converged, usually in 4–5 cycles.

The solution to this iterative loop yielded the smallest IC engine and gearbox required to meet the power needed to drive the electrical generator. Using the scaling principles from (14) and Fig. 12, the final mass of the IC engine and gearbox were computed. The mass of the gearbox and IC engine combined with the previously solved mass of the electrical generator yielded the minimal system mass of a generator to provide a given power. Note that this mass does not include fuel weight, which is included in later discussions of energy density.

4. Per-power comparison of generators to batteries

Once we understand the *smallest* mass generator that can supply a given power, we can compare the power of this generator to that of a battery, assuming fuel is available. As mentioned earlier, this study examined a common military battery used for mobile robotics and portable electronics, the BB2590 lithium ion battery. This battery system is designed for a maximum of 350 W power output and has a mass of approximately 1.4 kg [18]. The dotted line in Fig. 13 shows the generator mass relative to a BB2590 battery, assuming both provide an equivalent peak power output. One can immediately see that a generator, on a per-mass basis, will never be able to provide as much power as a lithium ion battery. Or more directly, a generator is always less "power dense" than a battery for the size scales appropriate to a robot.

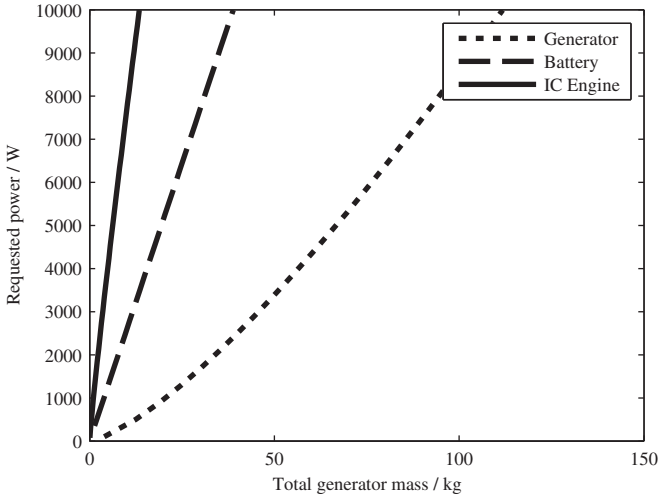

Fig. 13. Comparing peak power between generators and BB2590 batteries.

In contrast, the power per unit mass for IC engines, also shown in Fig. 13, is higher than that of a battery or generator. But when using an IC engine for locomotion, electricity must still be created to power supporting systems. Therefore, some type of generator would be required with the IC engine. Small IC engines are also known to have poor reliability due to high cycle rates.

A more appropriate analysis may be to compare a generator to a battery on a "per-energy" basis. To perform this analysis, first one must include the mass and energy content of fuel within the generator calculation. Next, one must assume an equivalent power output for both the generator and battery. For this study, the C10 power rating of a battery was used to determine the power of the equivalent generator. For example, a 10 A–h, 24 V battery with a C10 rating specifies that this battery produces power continuously at 1 amp, 24 V (thus 24 W), for 10 h. This C10 rating was also used to approximate the total energy output of the battery, as is typical for the A-h rating.

Assuming these power outputs of the generator, one can calculate the mass required for a generator with only the amount of fuel to achieve the equivalent energy of a BB2590 battery with the same power rating. Fig. 14 shows the resulting generator masses as a function of constant battery energy being replaced. Unlike power density, for a given energy level the generator becomes more efficient than the BB2590 as a power source. In Fig. 14 the horizontal line represents the energy of a single BB2590 battery. This line also happens to be close to the point where fuel-based generator systems become more efficient energy sources than batteries on a per-mass basis.

The generator is comprised of an IC engine, gearbox, DC motor, and fuel. When computing the total mass of the system, one must factor in an additional weight penalty to account for the additional casing required to support the generator and hold the fuel. This additional weight penalty can be hard to determine analytically, so for this study, a 25% additional mass was included as an approximation. The line in Fig. 15 represents the model-predicted generator mass as a function of power output of the generator. Each individual point on this chart represents actual electrical generators on the market, and thus the model shows very good agreement with vendor data.

Fig. 15 also shows that, for low-power generators, the model over-predicts the generator mass. For high-powered generators, the model under-predicts mass. The authors feel that this trend is because, within the model, the penalty function associated with the frame weight is a fixed fraction of the overall weight. Smaller generators hold less fuel and thus require less frame mass to contain all of the parts. Conversely, larger generators hold a greater amount of fuel and require more complex cooling systems, and thus require proportionally heavier cases, cooling fins, and in many instances wheels or other equipment to help move them. The penalty function associated with the generator casing is not adjusted with weight since these additional frame elements would not likely be necessary for a generator embedded within a robot.

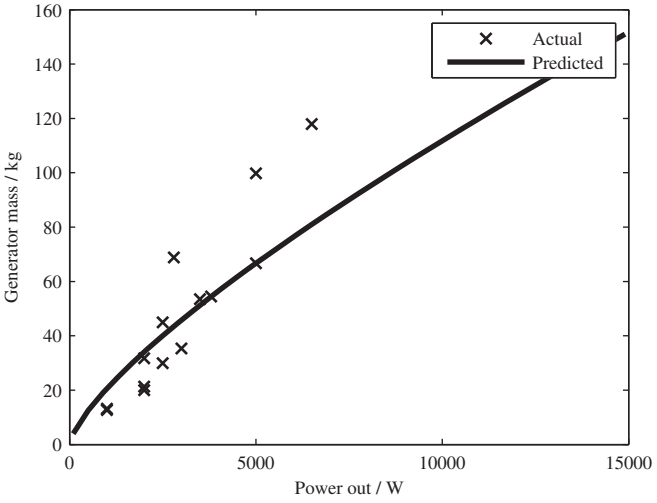

Fig. 15. Comparing predicted generator performance to vendor data.

5. Equivalent mass power sources

Once the generator models were confirmed with vendor data, the relationship between generator energy and size was sought on a per-mass basis. The goal of this analysis was to determine how the total energy and corresponding functional range of a robot would increase or decrease if batteries were replaced with a generator. Each circle in Fig. 16 represents the intersection point where the generator begins to have a higher energy density than a given battery chemistry. The generator first intersects lead acid, then

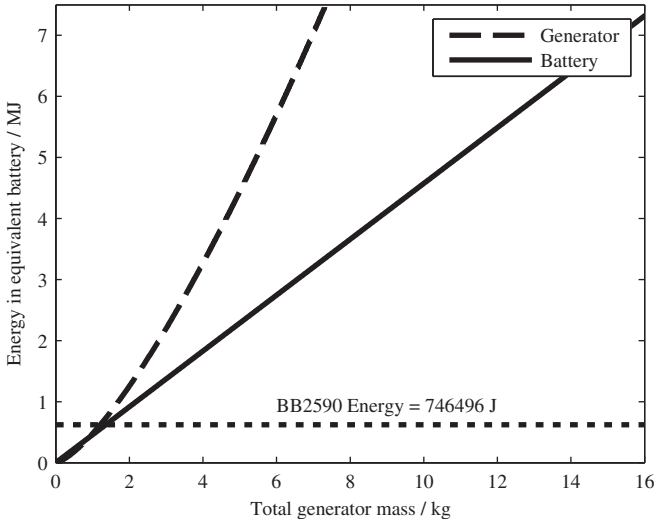

Fig. 14. Comparing the relative energy density of a generator and BB2590 batteries.

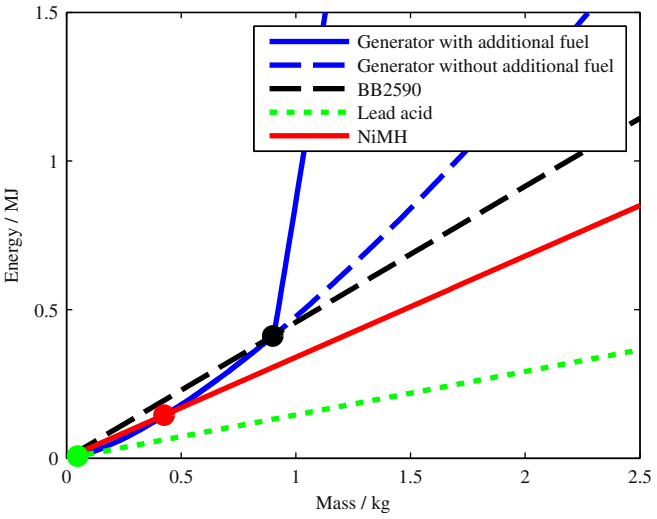

Fig. 16. Energy density of multiple power sources.

nickel metal hydride (NiMH), and finally lithium ion (Li-ion) in order of ascending energy density.

When comparing the performance of a generator to a battery, it is very limiting to assume that a generator has only the fuel equivalent to the battery it replaces. By relaxing this assumption, the benefit of using a generator becomes clear. Li-ion batteries, which have the highest energy density among commercial rechargeable batteries, will be used to explain this point. The intersection point between Li-ion batteries and generators occurs at the top right of Fig. 16. This intersection represents the point at which a generator is a more efficient source of energy than a battery on the basis of energy per unit mass. The generator equivalent mass line forks after this intersection point. The dotted line represents the mass of a generator to provide equivalent energy to that of a battery. The solid line represents the amount of energy a generator contains if any spare mass is dedicated to additional fuel. Since the energy density of the generator is greater than that of a battery beyond the intersection point, any mass savings is dedicated to additional fuel.

Fig. 16 shows that after some mass threshold, a generator will always achieve a higher energy density for a given constant power demand relative to a battery. The energy difference beyond that threshold is dramatic if the generator holds additional fuel. Conversely, it also shows that for current methods of generating power using DC motors, it does not make sense to use generator power topologies for smaller robots.

6. Inferring future trends

The intersection point determining the battery/generator tradeoff is not necessarily fixed because of assumptions in the development of generator scaling principles. Rather than defining a single intersection point, both additional generator casing mass and lithium ion energy density were varied to represent a working envelope as shown in Fig. 17. This envelope is represented as a shaded area with a dotted line border. For energy sources greater than 1.5 MJ a generator is a more effective energy source while below 0.2 MJ a battery is a preferable source of energy. Between 0.2 MJ and 1.5 MJ, the preferred energy source is more sensitive to the assumptions made and the design of the generator. The energy density of the Li-ion battery and the packaging mass of the generator components are the two attributes which can be varied to generate the working envelope in Fig. 17.

The first assumption which requires consideration is that the generator casing will add an additional 25% to the generator mass. This casing may have less or more mass than that assumed here. The downward pointing triangles in Fig. 17 represent the intersection point between BB2590 batteries with an energy density of 456 kJ kg^{-1} and generators that have casings that add 0, 25, 50, and 75% to the total mass of the generator [18]. As the casing mass of the generator increases from 0 to 75%, the intersection point shifts up and to the right. As expected, the greater the mass of the casing, the more a battery is favored as an energy source for larger robots.

The energy density of a BB2590 battery is represented by a dark, thicker, diagonal line in Fig. 17 [18]. This value is assumed to be near the optimal energy density for a military-grade robot battery. The performance of a commercially available battery is assumed to be represented by this line. A battery with a higher energy density would shift the location of the intersection point between batteries and the generator. The results of using a battery with a higher energy density are also shown in Fig. 17. The energy density of the Li-ion battery was increased from its current density, denoted as 100% in the figure above, to 130% of the energy density of a commercially available Li-ion battery.

The four additional lines in Fig. 17 represent the intersection points between batteries with energy densities of 100, 110, 120, and 130% of a BB2590 and a generator with a casing of 25% of the overall mass. As battery technology improves, the masses of the generator and fuel required to replace the battery increases. However, for robots that require more than 2.7 kg of battery power, it is also observed that it is unlikely a new battery will be better than a hybrid powertrain design, assuming reliability and cost is not of concern.

7. Combining power/energy requirements

As discussed in Section 5, there is a point at which generators become more efficient than batteries on the basis of energy per unit mass. Beyond this intersection, a generator will have less mass than a battery with equivalent energy storage. Fig. 16 shows that adding the difference in mass to the generator as extra fuel increases energy storage, but the peak power output of the generator is unchanged. If batteries are added to the generator instead of fuel, the peak power output increases. The results of this analysis are

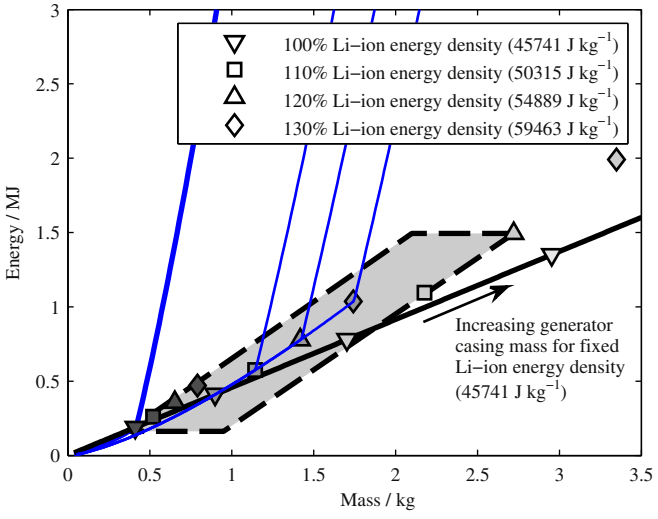

Fig. 17. Variation of parameters.

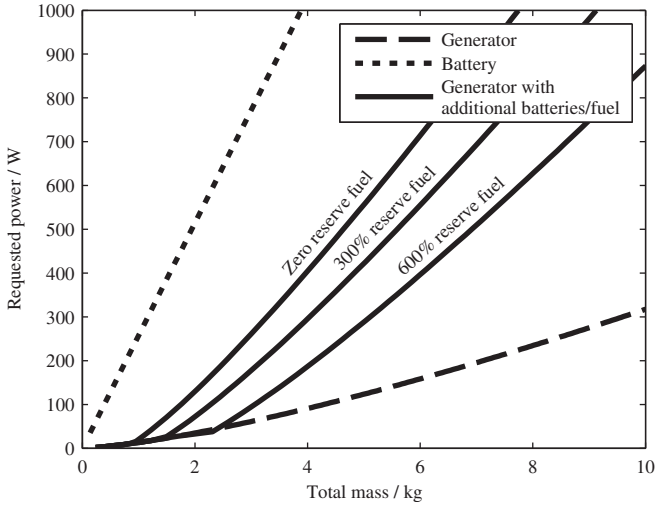

Fig. 18. Comparison of peak power output of battery and generator.

shown in Fig. 18, which is similar to Fig. 13 with the addition of the reserve fuel lines.

The zero reserve fuel line intersection occurs at the point where generators become more efficient than batteries from a specific energy (energy per unit mass) analysis. Points on the zero reserve fuel line represent the power output of a generator and battery system with a mass equal to that of a battery containing the same amount of energy as is available from the generator. The 300% and 600% reserve fuel lines are similar except the system consists of the generator, additional fuel, and a battery. The 300% reserve line represents enough additional fuel to provide four times the energy of an equivalent mass battery, and the 600% reserve line represents enough fuel to provide seven times the energy of an equivalent mass battery.

Fig. 18 is useful as a design tool when sizing power systems. For example, a system requiring 500 W of power would need a 1.9 kg battery, providing 870 kJ of energy. Another option would be a generator and battery system with 300% reserve fuel, weighing 6.5 kg but providing 25 MJ of energy.

8. Conclusion

This study presented an analysis of the size scaling of components present within a hybrid robot to determine the size scale at which generators are more suited than batteries on a power density and energy density basis. The process of allometric modeling of generators was introduced, and assuming a 25% weight penalty for the generator casing, the predicted generator performances versus mass compared favorably to published generator specifications. The specific power of a generator was found to never be greater than that of a battery or group of batteries. On an energy-per-mass basis, it was found that weight-optimized generators have an energy level substantially higher than that of a BB2590 battery pack with a mass of 0.9 kg or higher.

If a generator requires more infrastructure and casing weight than the 25% penalty assumed earlier, the allometry predicts that this change will shift the intersection point between batteries and generators to a higher mass. Increasing the specific energy of a battery above that of the lithium ion BB2590 battery used as a reference in this analysis also increases the mass at which batteries are more effective than liquid fuel sources. For modest improvements in battery and weight-reduction technology, it was found that generators will nearly always out-perform batteries on a per-energy and per-power basis if the batteries required weigh more than 2.7 kg.

Overall, the results of this work agree well with current trends in the automotive industry. Ground robot missions requiring small amounts of energy can be easily powered using batteries, which are quiet, clean, and easily rechargeable. Missions requiring large amounts of energy due to longer durations can be powered using a generator weighing much less than the equivalent energy stored in batteries. Analogously, automobile manufacturers develop hybrid vehicles which are able to run solely on batteries during short trips, but that utilize a generator to greatly improve the range of the vehicle.

Acknowledgment

This work was supported by the NAVSEA Contract Number N00024-D-02-D-6604, Delivery Order Number 0501. The content of the information does not necessarily reflect the position or policy of NAVSEA, and no official endorsement should be inferred.

References

[1] M. Fischer, M. Werber, P. Schwartz, Energy Policy 37 (2009) 2639–2641.
[2] J.-D. Nicoud, Int. Symp. Micro Machine Hum. Sci. (1995) 1–6.
[3] G. Caprari, T. Estier, R. Siegwart, J. Micromechatronics 1 (2001) 177–189.
[4] J. Madden, Science 318 (2007) 1094–1097.
[5] J. Marden, J. Exp. Biol. 208 (2004) 1653–1664.
[6] M. Ehsani, K. Rahman, IEEE Power Electronics in Transportation (1996) 49–56.
[7] Z. Rahman, M. Ehsani, K.L Butler, An investigation of electric motor drive characteristics for EV and HEV propulsion systems, 2000 SAE Future Transportation Technology Conf. Aug 21-23, 2000.
[8] M. Kim, H. Peng, J. Power Sources 165 (2006) 819–832.
[9] C. Lin, J. Kang, J. Grizzle, H. Peng, Energy management strategy for a parallel hybrid electric truck, 2001 American Control Conf., June 25-27, 2001.
[10] C. Lin, Z. Filipi, L. Louca, H. Peng, D. Assanis, J. Stein, Int. J. Veh. Des. 11 (2004) 349–370.
[11] Batteries vs generators, 02-22-2012, http://corrosion-doctors.org/Batteries/choice.htm.
[12] Comparing the battery with other power sources, 02-22-2012, http://batteryuniversity.com/learn/article/comparing_the_battery_with_other_power_sources.
[13] Pittman 9234S006 DC Motor Datasheet (PDF), 06-12-2011, http://automationexpress.com/Products/DC_Motors/pdf/9234S006.PDF.
[14] M. Caduff, M. Huijbregts, H. Althaus, A. Hendriks, Environ. Sci. Technol. 45 (2011) 751–754.
[15] T. Kenjo, S. Nagamori, Permanent-Magnet and Brushless DC Motors, Oxford University Press, Oxford, 1985.
[16] D. Clark, M. Owings, Building Robot Drive Trains, McGraw-Hill, 2002.
[17] T. McMahon, J. Bonner, On Size and Life, Scientific American Books, Inc., New York, 1983.
[18] M. Juzkow, J. Power Sources 80 (1999) 286–292.
[19] P. Flynn, et al., Meeting the Energy Needs of Future Warriors, The National Academies Press, Washington, DC, 2004.